

Green Chemistry

Accepted Manuscript



This article can be cited before page numbers have been issued, to do this please use: M. Joharian, A. Azhdari Tehrani, A. Morsali, L. Carlucci and D. M. Proserpio, *Green Chem.*, 2018, DOI: 10.1039/C8GC02367K.



This is an Accepted Manuscript, which has been through the Royal Society of Chemistry peer review process and has been accepted for publication.

Accepted Manuscripts are published online shortly after acceptance, before technical editing, formatting and proof reading. Using this free service, authors can make their results available to the community, in citable form, before we publish the edited article. We will replace this Accepted Manuscript with the edited and formatted Advance Article as soon as it is available.

You can find more information about Accepted Manuscripts in the [author guidelines](#).

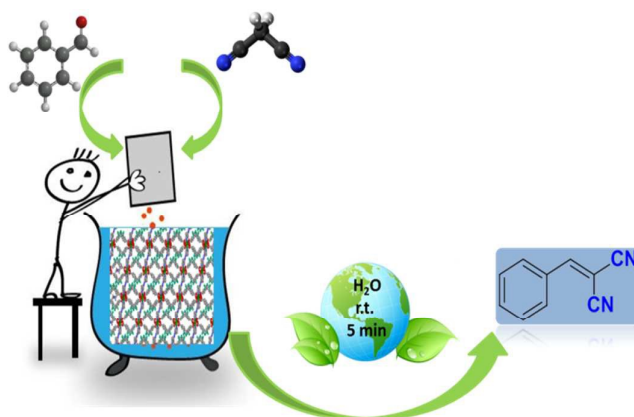
Please note that technical editing may introduce minor changes to the text and/or graphics, which may alter content. The journal's standard [Terms & Conditions](#) and the ethical guidelines, outlined in our [author and reviewer resource centre](#), still apply. In no event shall the Royal Society of Chemistry be held responsible for any errors or omissions in this Accepted Manuscript or any consequences arising from the use of any information it contains.

Water-Stable Fluorinated Metal–Organic Frameworks (F-MOFs) with Hydrophobic Properties as Efficient and Highly Active Heterogeneous Catalysts in Aqueous Solution

Monika Joharian^a, Alireza Azhdari Tehrani^a, Ali Morsali^{a*}, Lucia Carlucci^b, and Davide M. Proserpio^{b,c}

- ^a) Department of Chemistry, Faculty of sciences, Tarbiat Modares University, PO. BOX 14115-4838, Tehran, Iran.
^b) Dipartimento di Chimica, Università degli Studi di Milano, Via C. Golgi 19, 20133 Milano, Italy
^c) Samara Center for Theoretical Material Science (SCTMS), Samara State Technical University, Samara 443100, Russia.

E-mail: Morsali_a@modares.ac.ir



Abstract

Two new fluorinated metal–organic frameworks $[\text{Zn}_2(\text{hfipbb})_2(4\text{-bpdb})]\cdot 0.5\text{DMF}$ (TMU-55) and $[\text{Zn}_2(\text{hfipbb})_2(4\text{-bpdh})]\cdot 2\text{DMF}$ (HTMU-55) have been solvothermally synthesized by the reaction of two linear N-containing ligands as pillars (4-bpdb = 1,4-bis(4-pyridyl)-2,3-diaza-1,3-butadiene, 4-bpdh = 2,5-bis(4-pyridyl)-3,4-diaza-2,4-hexadiene), and a flexible V-shaped fluorinated linker, H_2hfipbb = 4,4'-(hexafluoroisopropylidene) bis(benzoic acid)). The two compounds were characterized by different techniques such as X-ray crystallography, powder X-ray diffraction (PXRD), infrared spectroscopy (IR), contact angle (CA), thermo gravimetry (TGA), field emission scanning electron microscope (FE-SEM), inductively coupled plasma (ICP), and Brunauer–Emmett–Teller (BET) surface area analysis. Both compounds are structurally similar and exhibit three dimensional (3D) coordination frameworks with hydrophobic properties. The catalytic activity of these isorecticular F-MOFs as efficient base heterogeneous catalysts toward Knoevenagel condensation reaction was tested and compared to each other. TMU-55 and HTMU-55 exhibited good catalytic activity (with a minimum amount of catalyst, 2.5 mg (0.5 mol%), and the shortest time, 5 min) in water media as a green solvent with excellent conversions. Also, the results were considerably higher in comparison with the most given values in the literature for this reaction at ambient temperature. The remarkable catalytic

performance of TMU-55 and HTMU-55 in water can be attributed to the presence of hydrophobic fluoro groups near the basic reaction center in the F-MOFs. These catalysts maintain their crystalline frameworks after the reaction and are easily recovered and reused at least for three cycles without significant loss in their catalytic activity. Furthermore, the conversion of benzaldehyde can be kept over 95% while the selectivity of the Knoevenagel reaction is kept at 100%.

Keywords

Heterogeneous catalyst; F-MOFs; Hydrophobicity; Knoevenagel condensation reaction.

Introduction

Metal-organic frameworks (MOFs) have emerged as a unique class of crystalline materials that have attracted tremendous attention due to their potential applications in different research areas such as gas storage, catalysis, drug delivery, sensing, and removal of hazardous materials [1-12]. The diverse number of organic ligands, inorganic metal ions/clusters, and guests were used to construct MOFs.

One of the especially interesting applications for MOFs is heterogeneous catalysis. In recent years, numerous studies have focused on heterogeneous catalyst based on MOFs owing to their high surface area, porosity, and chemical tunability [13]. Heterogeneous catalysis is superior to homogeneous catalysis in terms of reusability, easier separation, and waste minimization.

On the other hand, by introducing suitable catalytic sites into their structure, MOFs are the ideal candidates as heterogeneous catalytic materials for a wide range of reactions [14-17]. Two major parts in the MOFs which are very important in the catalytic behaviour, can serve as the active centers: unsaturated metal site as Lewis acid, and reactive functional groups attached to any components (linkers) of the frameworks. In order to have a catalytic material, the functional groups need to be free and available to the substrates and should not be directly coordinated to the metal ions of the MOFs.

A feature that has seldom been taken into consideration for improving catalytic activity of MOFs is hydrophobicity character of the pore surface. Recently, Farrusseng's research group attributed the increase in the reaction rate of the Knoevenagel condensation to the modification of the environment of the catalytic sites and, in particular, through the creation of a hydrophobic environment surrounding [18, 19].

The Knoevenagel condensation is a reaction between an active methylene compound and a carbonyl compound (aldehydes or ketones). It is the most popular reaction used to investigate coordination polymers and MOFs containing basic functionalized structures. Furthermore, it

is one of the most important reactions for the formation of C=C bond, for the synthesis of several fine chemicals and medical intermediates, In general, it is a highly useful reaction in synthetic chemistry [20-28].

Despite various solid catalysts have been employed for the Knoevenagel condensation reaction, such as mesoporous materials [29-31], ionic liquids [32,33], organometallic catalysts [34], zeolites [35,36], etc. only few sustainable methods that utilize basic heterogeneous catalyst were reported [37]. However, most of these methods have significant drawbacks, such as using hazardous and carcinogenic solvents, high catalyst loading or non-recoverable catalysts that sometimes contain toxic metals. Therefore, there is a great need for new catalytic methods that do not have these problems.

Hence, further development of appropriate and more impressive heterogeneous catalysts for the Knoevenagel reactions is essential. There have been many reports with MOFs as superior heterogeneous catalysts for Knoevenagel condensation [38-40] and also MOFs with basic groups such as azine are efficient catalysts for this reaction [28]. Most of the MOFs that have been investigated in Knoevenagel condensation reaction are not stable in water and need high temperature, high amount of catalyst or more time to complete the reaction. So we pursued the development of more suitable MOFs as catalysts for this reaction. To overcome these issues, we pursued the development of more suitable MOFs as catalysts for this reaction.

Recently researchers have paid attention to the possibility of synthesizing fluorinated metal-organic frameworks (F-MOFs) as a new class of advanced porous material. Compared to metal-organic frameworks, F-MOFs with fluorinated channels or cavities are expected to have increased catalytic activity, thermal stability, higher gas affinity and selectivity, etc. [41, 42]. It is generally acknowledged that fluorination can make a diversity of new properties to MOFs, such as enhanced hydrophobicity, super acidity, low surface energy, and excellent optical and electrical properties [41]. Hydrophobicity, through the presence of alkyl or fluorinated (F, CF₃,...) groups, is also an efficient way to improve the water stability of MOFs. Therefore we tried to synthesize such novel F-MOFs based on fluorinated groups and to evaluate their properties of F-MOFs in the catalytic reaction in the presence of water as an interesting issue.

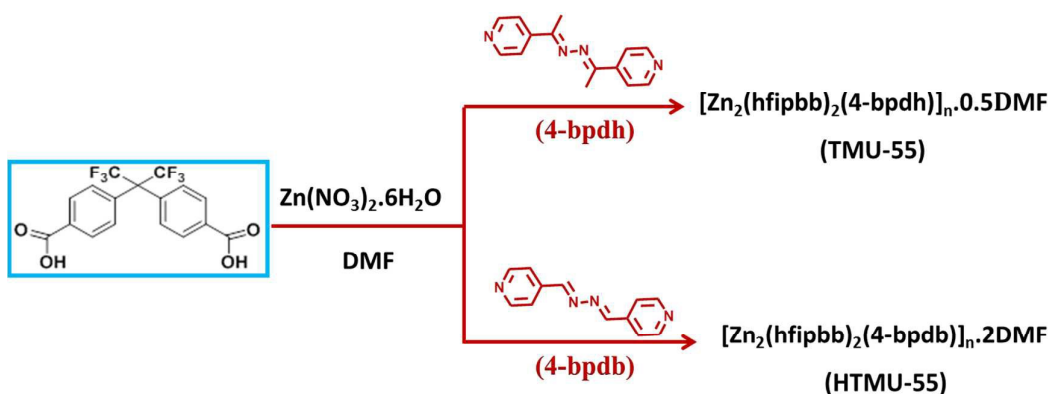
Among various ligands, 4,4'-(hexafluoroisopropylidene) bis(benzoic acid) (H₂hfipbb) as a semi-rigid and long dicarboxylate ligand has been investigated for its bent geometry and hydrophobic features. The -CF₃ terminated surface was reported to possess low free energy and the best hydrophobicity [43, 44], hence MOFs constructed from the H₂hfipbb ligand may

have hydrophobic features and better water stability [45], potential applications in hydrophobic materials.

In this work, we have focused on the synthesis of two pillared F-MOFs from 4-bpdb = 1,4-bis(4-pyridyl)-2,3-diaza-1,3-butadiene, 4-bpdh = 2,5-bis(4-pyridyl)-3,4-diaza-2,4-hexadiene, and the flexible fluorinated dicarboxylate building block, H₂hfipbb= 4,4'-(hexafluoroisopropylidene) bis (benzoic acid) (Scheme 1) to obtain novel, highly efficient, stable, and recyclable Zn based heterogeneous catalysts. The incorporation of such hydrophobic organic linker in the MOFs structures, may also serve to develop heterogeneous organocatalyst with good water stability and high catalytic activity in aqueous solution.

Because the Knoevenagel reaction occurs with basic catalysts we wish to use TMU-55 and HTMU-55 (TMU corresponds to Tarbiat Modares University) containing azine groups as efficient heterogeneous catalysts.

Based on this assumption, the catalytic behaviour of these hydrophobic frameworks for the Knoevenagel condensation reaction of carbonyl compounds with malononitrile in the presence of water as the appealing idea was investigated. Interestingly, high catalytic activities were observed even with minimum amount of F-MOFs and at room temperature, as well as, good reusability of the catalyst without significant degradation in activity. Moreover, the utilization of harmful solvents was avoided and solvents were environmentally friendly.



Scheme 1. Synthetic details of the two F-MOFs obtained with the use of zinc salt in combination with H₂hfipbb and 4-bpdh and 4-bpdb linkers.

2. Experimental

2.1. Materials and measurements

All starting materials and solvents for the synthesis and analysis were commercially available from Aldrich and Merck Companies and used as received. The ligands 1,4-bis(4-pyridyl)-2,3-diaza-1,3-butadiene (4-bpdb) and Ligand 2,5-bis(4-pyridyl)-3,4-diaza-2,4-hexadiene (4-bpdh) were prepared by the reported method [46].

IR spectra were recorded using a Nicolet Fourier Transform IR, Nicolet 100 spectrometer in the range 500-4000 cm^{-1} using the KBr disk technique. The inductively coupled plasma (ICP) analyses were performed on a Varian ICP-OES VISTA-PRO CCD instrument. Melting points were measured on an Electrothermal 9100 apparatus. The thermal behaviour was measured with a PL-STA 1500 apparatus with the rate of $10^\circ\text{C}\cdot\text{min}^{-1}$ in a static atmosphere of argon. Gas chromatography (GC) runs were performed on an Echrom GC A90 gas chromatograph. The samples were also characterized by a field emission scanning electron microscope (FE-SEM) TESCAN MIRA with gold coating. X-ray powder diffraction (PXRD) measurements were performed using a Philips X'pert diffractometer with monochromated Cu-K α ($\lambda = 1.54056 \text{ \AA}$) radiation. The contact angle was measured by an OCA 15 plus apparatus.

X-ray diffraction structure determinations:

Single crystal of TMU-55 was selected and mounted in inert oil and transferred to the cold gas stream of a Bruker APEX-II CCD diffractometer. The data were corrected for absorption based on the multi-scan technique as implemented in SADABS. The structures were solved by conventional methods and refined using SHELX2016 [47] implemented in WinGX graphical user interface [48]. Anisotropic thermal parameters were refined for non-hydrogen atoms and hydrogen atoms were calculated and refined with a riding model. A DMF molecule was refined as disorder model on a 2-fold axis. CCDC 1852195 contains the supplementary crystallographic data for this paper. These data can be obtained free of charge from The Cambridge Crystallographic Data Center via http://www.ccdc.cam.ac.uk/data_request/cif.

2.2. Synthesis of $[\text{Zn}_2(\text{hfipbb})_2(4\text{-bpdh})].0.5\text{DMF}$ (TMU-55) and $[\text{Zn}_2(\text{hfipbb})_2(4\text{-bpdb})].2\text{DMF}$ (HTMU-55)

To prepare the single crystals of TMU-55 and HTMU-55, at first H_2hfipbb (0.039 g, 0.1 mmol), 4-bpdh (0.024 g, 0.1 mmol) or 4-bpdb (0.021 g, 0.1 mmol), $\text{Zn}(\text{NO}_3)_2 \cdot 6\text{H}_2\text{O}$ (0.03 g, 0.1 mmol) and N,N-dimethylformamide (DMF; 20 ml), were mixed. Then the solution was

divided into 3 ml glass vials and each filled up to 2.5 ml. The vials were closed tightly and set in an oven and heated for 3 days at 80°C. After the crystals were formed, they were recovered by filtration and dried at 80°C in an oven overnight. Yield: 83% for TMU-55 and 81% for HTMU-55 (scheme 1).

Selected IR peaks (cm^{-1}) for TMU-55: 3082(w), 2929(w), 1687(s), 1641(vs), 1562(m), 1404(vs), 1247(s), 1212(w), 1170(m), 964(m).

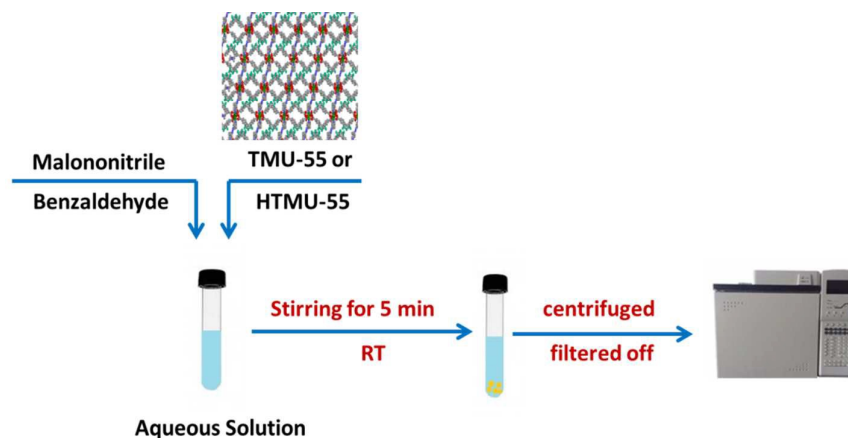
Selected IR peaks (cm^{-1}) for HTMU-55: 3076(w), 2931(w), 1686(m), 1639(s), 1563(m), 1499(w), 1406(s), 1248(m), 962(m).

2.3. Activation method

Before catalysis process, for removing guest DMF molecules, the crystals were immersed in 5 ml of CH_3CN for 3 days and fresh CH_3CN added every 24 h. After 3 days the CH_3CN solution was decanted and dried at 80°C at least for 12 h.

2.4. Catalytic experiments

As shown in Scheme 2 catalytic experiments were carried out in a 5-ml capped glass tube. In a typical procedure for the Knoevenagel reaction, 0.5 mmol of malononitrile, 0.2 mmol of an aromatic ketone; cyclohexanone, and four aldehyde compounds; benzaldehyde, 4-Methylbenzaldehyde, 4-Nitrobenzaldehyde, 4-Methoxybenzaldehyde, 4-Chlorobenzaldehyde, and 2.5 mg of activated catalyst were added in 3 mL of different solvents (Scheme2). The resulting mixture was stirred at room temperature for 5 min. Gas chromatography (GC) analysis was employed to detect the reaction progress and catalytic activity. When the reaction was completed, the catalyst was recovered by centrifugation, while the supernatant reaction mixture was passed through a 0.4 μ filter and subsequently analyzed with GC apparatus. The condensation products were identified by comparison of their retention times with those of authentic samples. The conversions are based on the starting substrates. The results were summarized in (Figures S4-S6 and Tables 1,2).



Scheme 2. Schematic representation of the Knoevenagel condensation reaction.

3. Results and discussion

Crystal Structure Analysis

HTMU-55 and TMU-55 were synthesized using the solvothermal method by simply mixing $\text{Zn}(\text{NO}_3)_2 \cdot 6\text{H}_2\text{O}$ and H_2hfipbb with 4-bpdb and 4-bpdh ligands, respectively. Crystal structure of HTMU-55 has been confirmed by comparison of powder pattern with the calculated from the known structure (HUQFEG) [49]. Single crystal X-ray analysis of TMU-55 reveals that it is isorecticular with HTMU-55 and HUQFEG. TMU-55 $[\text{Zn}_2(\text{hfipbb})_2(4\text{-bpdh})] \cdot 0.5\text{DMF}$ crystallizes in the monoclinic $C2/c$ space group. Crystal data with data collection and refinement parameters are summarized in Table S1, selected bond distances and bond angles are given in Table S2.

The Ortep view of the asymmetric unit, consisting of one zinc atom, one hfipbb and half 4-bpdh is reported in Figure 1a. The coordination geometry around Zn(II) can be described as distorted square pyramidal with the five coordination sites occupied by four oxygen atoms of carboxylate groups from hfipbb ligands and one pyridyl nitrogen atom from the 4-bpdh ligand (Figure 1b). The 3D framework is constructed from paddle-wheel $\text{Zn}_2(\text{COO})_4$ clusters bridged by hfipbb bent ligands to form a 2D square grids (**sql**) further connected by the pillar ligands (4-bpdh) (Figure 1c). About the Zn atom, the four O atoms are approximately in a plane, the Zn-O lengths are in the range 2.043(2)-2.048(2) Å, and Zn-N length is 2.026(2) Å. The Zn...Zn distance across the 4-bpdh ligand is 15.2 Å.

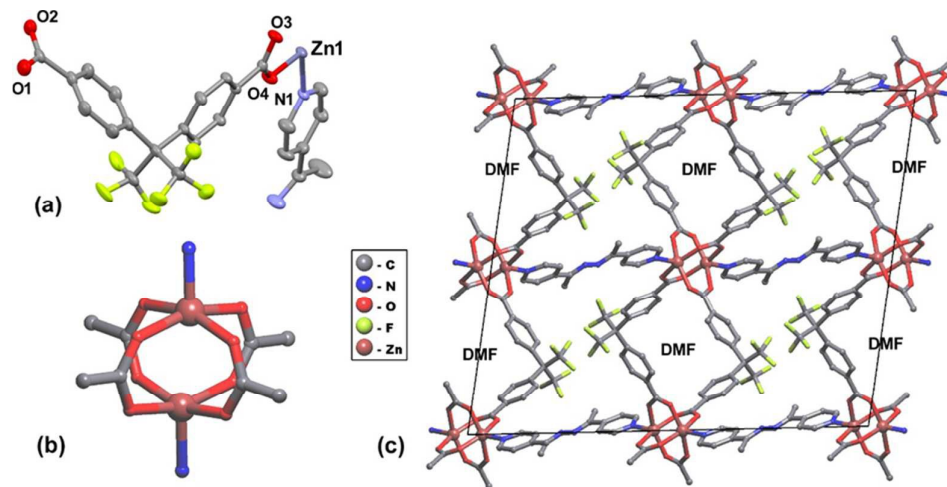


Fig 1. Crystal structure of $[Zn_2(hfipbb)_2(4-bpdh)].0.5DMF$ (TMU-55): (a) Ortep view of the asymmetric unit. (b) $\{Zn_2\}$ paddlewheel building unit. (c) View along the crystallographic b -axis showing the disposition of the clathrate DMF molecules along the helical channels.

Topological analysis [50] reveals a six-coordinated underlying net [51] formed by the zinc paddlewheel as 6-coordinated SBU and the two different ligands as 2-coordinated linkers. The single 3D framework is the rare self-catenated 6T9 net with $(4^4.6^{10}.8)$ point symbol. The 6T9 topology, according to ToposPro database [52], is observed only in 13 isorecticular structures, including HUQFEG. Ten of them have the same formula and SBUs as TMU-55 with M metals as Zn, Cu, Co, Cd, bent ligands such as hfipbb and oba (4,4'-oxybisbenzoate) [49, 53-61]. Moreover, the unit cell parameters are very similar and all crystallize in the same monoclinic $C2/c$ space group, showing a strong propensity toward 6T9 net.

The structure is formed by 2-fold interpenetrated square layers of $Zn_2(hfipbb)_2$ that stack along $[100]$ as ABAB. The interpenetration of the **sql** layers [62] is well known and frequently observed only for bent ligands [63]. Each single **sql** motif forming the 2-fold interpenetration (**sql(a)** and **sql(b)**) is connected above and below via the linear 4-bpdh or 4-bpbd ligands in a way to obtain a single underlying net: **sql(a)**-(ligand)-**sql(b)**. This convert the 2-fold 2D interpenetration in the resulting single 3D self-catenated net called 6T9 (Figure 2).

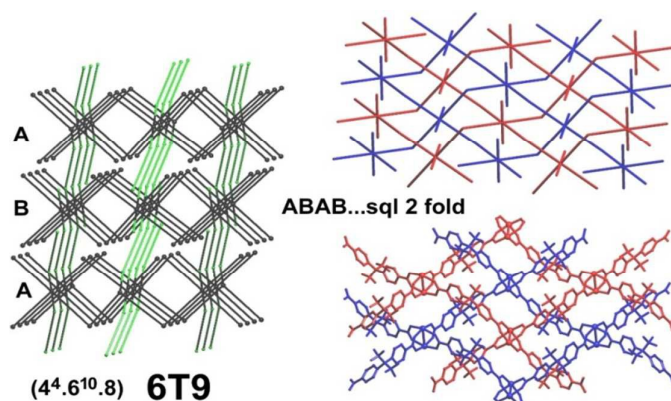
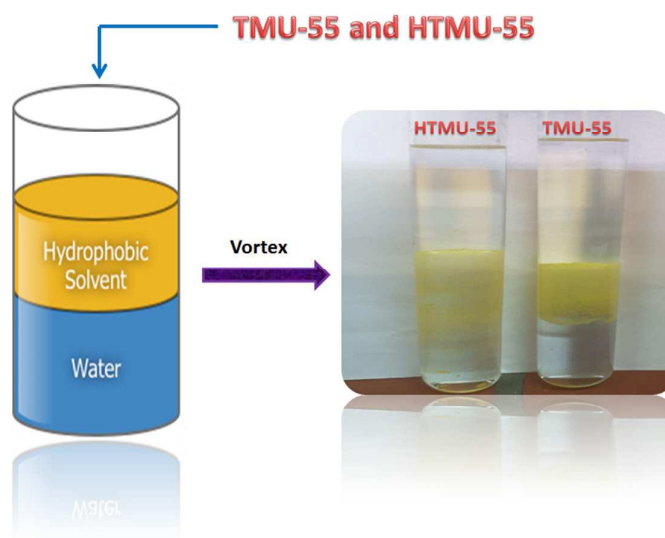


Fig 2. Topology of $[\text{Zn}_2(\text{hfipbb})_2(4\text{-bpdh})].0.5\text{DMF}$ (TMU-55). Left: view of the underlying self-interpenetrated 6T9 net where the simplified 2-fold interpenetrated **sql** layers (black) are connected by 4-bpdh ligand (green). Right: molecular (bottom) and simplified (top) views of the 2-fold interpenetrating **sql** layers (in red and blue) in TMU-55.

The structure shows narrow 1D channels along the crystallographic *b*-axis (Figure 1c) filled with guest solvent molecules (DMF for TMU-55 and water for HUQFEG). The walls of the channels are formed by double $\text{Zn}_2(\text{hfipbb})$ helices arising from the 2-fold **sql**.

Powder X-ray diffraction (PXRD) of TMU-55 and HTMU-55 confirms they are similar to each other and establishes their isomorphism and isoreticularity (Figure S1). Therefore, two basic azine- functionalized F-MOFs were synthesized which are different in terms of structural hydrophobicity (Scheme 3).

TMU-55 shows limited porosity with the calculated void space per unit cell for the guest-free framework of 14.5%. TMU-55 has 1D narrow channels with approximately $1.8 \times 3.3 \text{ \AA}$ in cross-section (including van der Waals radii) that is not large enough to be, in principle, accessible for N_2 (kinetic diameters for N_2 : 3.75 \AA) adsorption. Also, the BET measurement shows that HTMU-55 is nonporous toward N_2 .



Scheme 3. Schematic representation of structural hydrophobicity

To confirm and evaluate the hydrophobicity of these F-MOFs, Contact Angles were measured and analyzed. Such experiments show that both F-MOFs have relatively hydrophobic structures due to the presence of the fluoro groups in their structures (TMU-55: 71.55 and HTMU-55: 65.6 degrees). Moreover, TMU-55 has more hydrophobic character than HTMU-55 due to the incorporation of methyl groups (Figure S2).

In order to activate the potential interacting sites of the frameworks, the DMF molecules within the structure could be exchanged with acetonitrile molecules, which are more easily removed. The as-synthesized crystals of these frameworks were activated by solvent exchange with acetonitrile for 3 days. Then, the samples were filtered and dried at 80°C for 4 h. FT-IR spectroscopy (Figure 3) confirmed the removal of guest DMF molecules accommodated in the pores of the frameworks due to disappearance of the DMF peak at 1687 cm^{-1} . Powder X-ray diffraction (PXRD) (Figure 4) showed that the structures were retained after activation. The only places available and active for catalytic reaction are the basic nitrogen centers emerged within the F-MOF structure walls on the surface.

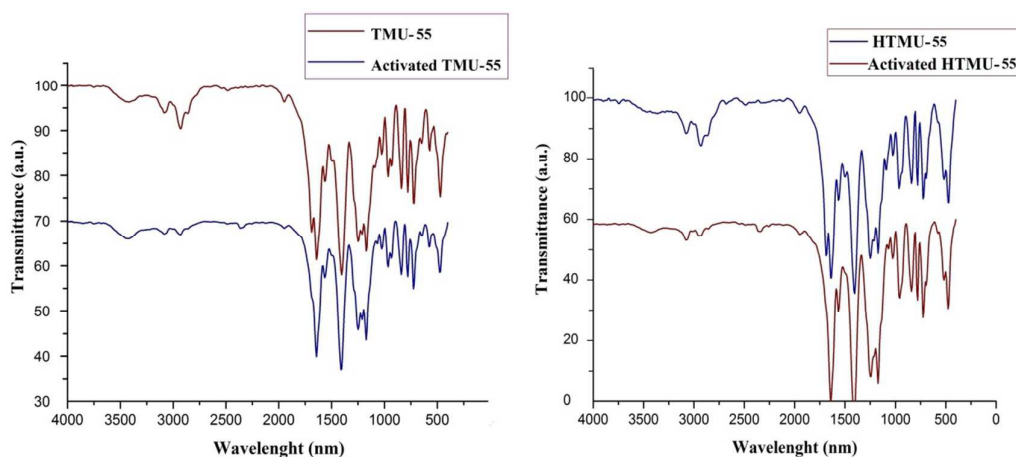


Fig 3. FT-IR spectra of as-synthesized by solvothermal method (in red) and of activated samples (in blue) for TMU-55 (left) and HTMU-55 (right).

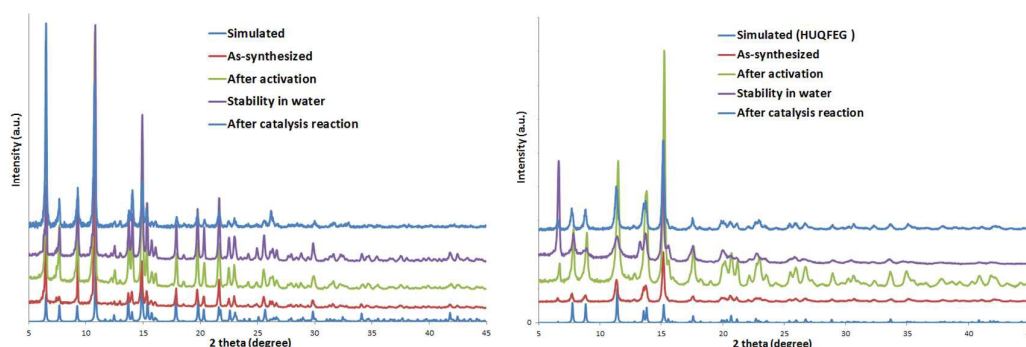


Fig4. Simulated and experimental PXRD patterns for as-synthesized, activated, treated in water, used as catalyst samples of TMU-55 (left) and HTMU-55 (right). We used HUQFEG structure to simulate the spectrum for HTMU-55.

As shown in Figure S3, thermogravimetric analysis (TGA) has been carried out in the range of 25–800 °C. TGA curve of TMU-55 exhibits a first weight loss, from room temperature up to 200 °C of 3.16%, that could be associated to the loss of 0.5 DMF molecule, a second weight loss in the temperature range of about 370–470 °C that refers to the degradation of the framework (62.08%), and finally, a complete decomposition of the compound to ZnO (Figure S3). The TG analysis of HTMU-55 shows a curve similar to that of TMU-55 apart for a more evident weight loss at the first step (from 25 to 200 °C) of 10.94% that can be attributed to the loss of 2 DMF molecules. The degradation of the framework (weight loss of 53.58%) is complete within 470 °C giving a final residue of ZnO (Figure S3).

Water Stability of F-MOFs

F-MOFs exhibiting stability in water have several potential applications as hydrophobic materials [64]. In this work, the stability of TMU-55 and HTMU-55 in water was investigated. The powder of these frameworks was immersed in water with vigorous stirring in a screw-capped glass vial for 3 d, after which PXRD analysis of the isolated sample revealed retention of the original framework structure (Figure 4). This remarkable water stability of F-MOFs could be attributed to the hydrophobic nature of the framework surface due to the CF_3 groups [45, 47, 65].

Catalytic studies

The application of MOFs in heterogeneous catalysis is one of the most widely investigated topics and is of great interest for the researchers. Many studies were performed on the heterogeneous catalysts including MOFs for the Knoevenagel condensation reaction. This condensation is usually catalyzed by Lewis bases or acids. The design and synthesis of non-toxic, reusable, easily separable, and low-cost catalysts has become an important area of research in the field of green chemistry.

In the present study, the Knoevenagel condensation reaction was chosen as a probe to study the catalytic activity of the compounds $[\text{Zn}_2(\text{hfipbb})_2(4\text{-bpdh})].0.5\text{DMF}$ (TMU-55) and $[\text{Zn}_2(\text{hfipbb})_2(4\text{-bpdb})].2\text{DMF}$ (HTMU-55).

The Knoevenagel condensation reaction is well known, not only as a weak base catalyzed model reaction but also as a reaction that generates a $\text{C}=\text{C}$ bond (Scheme S1).

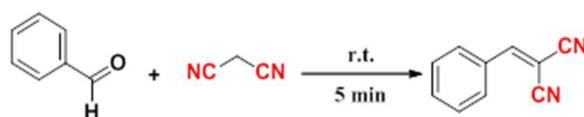
Using the suitable solvent can significantly increase the yield of the reaction. So in the first step of our experiments, in order to optimize the reaction solvent, a range of solvents was selected (Figure S4). In the experiments were employed 2.5 mg catalyst, 0.2 mmol of benzaldehyde and 0.5 mmol of malononitrile in 3 ml different solvents such as methanol, ethanol, H_2O , and toluene at room temperature. It can be concluded from these results that higher yields were achieved in polar protic solvents, while the reaction occurred with difficulty in solvents with the lower polarity such as toluene.

To reach high yield the Knoevenagel condensation reaction in H_2O was selected as a probe reaction.

The reaction with benzaldehyde in H_2O and in the absence of catalyst gave 5% conversion as obtained by GC (Table 1). Whereas in the presence of 2.5 mg TMU-55 and HTMU-55 as the catalyst for 5 min at room temperature, the reaction proceeded with 99% and 87% conversions, respectively. This observation clearly revealed the catalytic effect of the

synthesized F-MOFs. In addition, the same reaction runs were performed for optimization of the catalyst amounts. Malononitrile (0.5 mmol), benzaldehyde (0.2 mmol) and H₂O (3 mL) were mixed into three glass vessels equipped with a magnetic stirrer bar. Then 1, 2, and 2.5 mg of catalysts were added to each vessel, respectively. Reactions were monitored by GC (results are shown in Figure S5). During the survey of the reaction conditions, the best results were obtained by using 2.5 mg of the catalysts at r.t in 3 ml of H₂O.

Table 1. Knoevenagel condensation reaction performed in the presence of the two isorecticular F-MOFs catalysts (TMU-55 and HTMU-55) and in their absence.



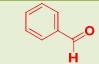
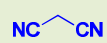
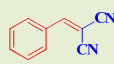
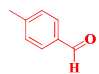
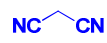
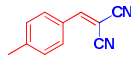
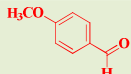
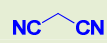
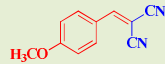
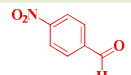
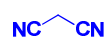
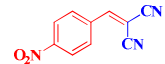
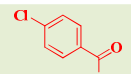
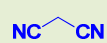
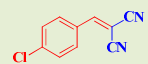
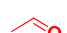
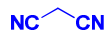
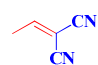
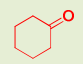
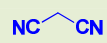
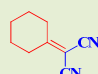
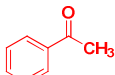
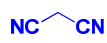
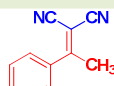
Entry	catalyst	Conversion (%)
1	TMU-55	99
2	HTMU-55	87
3	-	5

GC yield, Reaction conditions: benzaldehyde (0.2 mmol), malononitrile (0.5 mmol), 2.5 mg (0.5 mol%) catalyst, solvent: H₂O (3ml), r.t, 5 min.

The evaluation of the conversions with the selectivity 100% in all cases show that only one product is formed. Any intermediate of the condensation reaction or any side products were not observed.

We used various ketones and also aldehydes as substrates to compare the catalytic activity of the F-MOFs in the presence of electron-donating or withdrawing groups. Results showed that the catalytic activity was enhanced by increased N-donor ligands basicity (Table 2 and Figure S6). In most of the papers for the Knoevenagel reaction, the reaction of aldehydes, such as benzaldehyde derivatives, is investigated because the ketones were reacted with malononitrile in more severe conditions.

Table 2. Knoevenagel condensation reaction catalyzed by the two isorecticular F-MOFs catalysts (TMU-55 and HTMU-55) in the presence of different aldehydes and ketones.

Entry	Catalyst	Substrate	Substrate	Product	Conversion (%)
1	TMU-55				99
	HTMU-55				87
2	TMU-55				71
	HTMU-55				59
3	TMU-55				65
	HTMU-55				50
4	TMU-55				100
	HTMU-55				91
5	TMU-55				99
	HTMU-55				90
6	TMU-55				67
	HTMU-55				52
7	TMU-55				61
	HTMU-55				48
8	TMU-55				59
	HTMU-55				47

GC yield, Reaction conditions: substrates (0.2 mmol), malononitrile (0.5 mmol), 2.5 mg (0.5 mol%) catalyst, solvent: H₂O (3ml), r.t, 5 min.

In addition, these catalyst F-MOFs can be recycled and are reused at least for 3 runs without significant loss of their efficiency. The reason for the 8% decreasing of the percentage of the conversion after the third run is most probably the deactivation of the active sites. The destruction of the structure it is unlikely to happen before the fourth reaction run as shown by PXRD and ICP (Figure 5). Leaching test was carried out for the zinc ions by ICP analysis and was found that less than 1% of the zinc atoms from the frameworks pass into the reaction solution, thus more than 99% of the zinc metal center does not leach into the reaction mixture during the reaction conditions. So these analyses prove the stability of the base catalyst during the reaction in the H₂O solvent. Moreover, the Zn species leached out from the solid are not able to catalyze the condensation on their own, a test with zinc (II) nitrate salts gives only 30% conversion in 4h. Also we test the residual activity of the solution without the solid and the reaction continues very slowly.

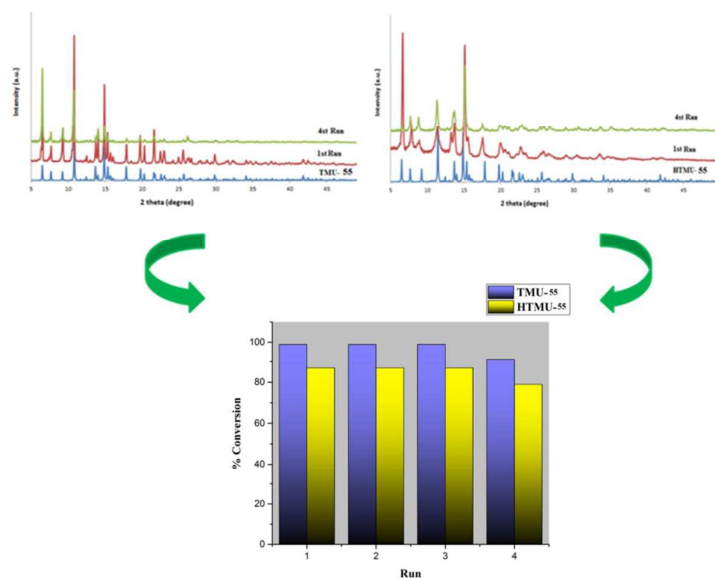


Fig 5. PXRD patterns of simulated and after the first and fourth catalytic cycle of TMU-55 (top left) and HTMU-55 (top right). On the bottom, bar chart (blue for TMU-55, yellow for HTMU-55) of the GC % conversion yield in the four catalytic cycles for the reaction conditions: benzaldehyde (0.2 mmol), malononitrile (0.5 mmol), 2.5 mg (0.5 mol%) catalyst, solvent: H₂O (3ml), r.t, 5 min.

SEM images taken on crystals of the two F-MOFs before and after a catalytic cycle, shown in Figure S7, indicate the maintenance of the frameworks after the Knoevenagel condensation reaction.

A comparison of the catalytic activity of TMU-55 and HTMU-55 with that of other heterogeneous catalysts previously used in such reaction is reported in Table 3. To demonstrate the advantages of our catalyst over other heterogeneous catalysts used in the Knoevenagel condensation reaction between benzaldehyde and malononitrile, we compared the obtained results based on the amount of catalyst, solvent used, and the reaction time (Table 3).

The results obtained in this work were considerably higher in comparison with the most given values in the literature for this reaction conducted at ambient temperature.

In this case, the reaction well proceeds in H₂O solvent through the role of hydrophobic groups (CF₃) over the hfipbb ligands. Results show that TMU-55 due to methyl groups near the basic center reaction in 4-bpdh ligand increases basicity and hydrophobicity and better interaction between azine groups (as Lewis base) in catalyst and substrate so has higher catalytic activity than HTMU-55 in aqueous media.

Table 3. A comparison of catalytic activity of various catalysts in the Knoevenagel condensation reaction of benzaldehyde and malononitrile.

Entry	Catalyst	Amount	Time	Solvent	Temp. [°C]	Conversion (%)	Ref.
1	Pb(cpna) ₂ .2DMF.6H ₂ O	3 mol%	24 h	CH ₃ CN	r.t.	100	66
2	[Cd(4-btapa) ₂ (NO ₃) ₂].6H ₂ O.2DMF	5 mol%	12 h	C ₆ H ₆	r.t.	98	67
3	[Cd(bipd) ₂ (DMF) ₂].(ClO ₄) ₂ .(2DMF)	4 mol%	30 min	C ₆ H ₆	r.t.	93	68
4	[Gd ₂ (tmbd) ₃ (DMF) ₄].4DMF.3H ₂ O	10 mol%	20 min	C ₆ H ₆	r.t.	96	69
5	Au@Cu(II)-MOF(1)	3 mol%	23 h	Toluene/ MeOH	r.t.	99	70
6	{[Ni ₃ (TBIB) ₂ (BTC) ₂ (H ₂ O) ₆].5C ₂ H ₅ OH·9H ₂ O} _n	5 mol%	2h	DCM	60 °C	100	71
7	Fe ₃ O ₄ @ZIF-8	4 mol%	3h	Toluene	r.t.	94	72
8	TMU-55	0.5 mol%	5 min	H ₂ O	r.t.	99	This work
9	HTMU-55	0.5 mol%	5 min	H ₂ O	r.t.	87	This work

4. Conclusion

Two new three dimensional isorecticular F-MOFs [Zn₂(hfipbb)₂(4-bpdh)].0.5DMF (TMU-55) and [Zn₂(hfipbb)₂(4-bpdb)].2DMF (HTMU-55) with different pillars and hydrophobic structures were solvothermally synthesized and characterized by different techniques. These F-MOFs were used as new solid base catalysts in the Knoevenagel condensation reaction given the basic character of the N-donor pillar ligands. The catalytic reaction proceeds well in aqueous media as a green solvent thanks to the hydrophobic groups (CF₃) of the hfipbb ligand. The two F-MOFs exhibit good catalytic activity with excellent conversions even in water at room temperature using low amount of catalyst (0.5 mol%) and short reaction time (5 min).

The better catalytic activity of TMU-55 is attributed to the presence of the methyl groups on the N basic centers in 4-bpdh that enhance the basicity and hydrophobicity of the nitrogen active centers. This study demonstrates the important role of the basicity of azine functionalized frameworks, as well as that of the hydrophobicity of the frameworks on the catalytic performance.

Acknowledgment

Support of this investigation by Tarbiat Modares University is gratefully acknowledged. L.C. and D.M.P thank Università degli Studi di Milano (Piano di Sviluppo di Ateneo, azione B, progetti di interesse interdisciplinare PSR2015-1716FDEMA_07) for financial support.

References

1. H. Furukawa, K. E. Cordova, M. O’Keeffe, O. M. Yaghi, *Science*. 2013, **341** (6149), 1230444.
2. A. R. Millward, O. M. Yaghi, *J. Am. Chem. Soc.* 2005, **127** (51), 17998-17999.
3. A. Corma, H. Garcia and F. X. Llabres I Xamena, *Chem. Rev.* 2010, **110**, 4606-4655.
4. L. Zhu, X.-Q. Liu, H.-L. Jiang, L.-B. Sun, *Chem. Rev.* 2017, **117** (12), 8129-8176.
5. H. Ghasempour, A. Azhdari Tehrani, A. Morsali, J. Wang, P. C. Junk, *CrystEngComm*. 2016, **18** (14), 2463-2468.
6. M. X. Wu, Y. W. Yang, *Adv. Mater.* 2017, **29**, 1606134.
7. W. P. Lustig, S. Mukherjee, N. D. Rudd, A. V. Desai, J. Li, S. K. Ghosh, *Chem. Soc. Rev.* 2017, **46** (11), 3242-3285.
8. Y. Peng, H. Huang, Y. Zhang, C. Kang, S. Chen, L. Song, D. Liu, C. Zhong, *Nature Commun.* 2018, **9** (1), 187.
9. J. B. DeCoste, G. W. Peterson, *Chem. Rev.* 2014, **114** (11), 5695-5727.
10. A. Azhdari Tehrani, L. Esrafil, S. Abedi, A. Morsali, L. Carlucci, D. M. Proserpio, J. Wang, P. C. Junk, and T. Liu, *Inorg. Chem.* 2017, **56** (3), 1446–1454.
11. X. Wang, W. Chen, L. Zhang, T. Yao, W. Liu, Y. Lin, H. Ju, J. Dong, L. Zheng, W. Yan, X. Zheng, Z. Li, X. Wang, J. Yang, D. He, Y. Wang, Z. Deng, Y. Wu, and Y. Li, *J. Am. Chem. Soc.* 2017, **139**, 9419-9422.
12. F. Xie, Q.-H. Chen, R. Xie, H.-F. Jiang, and M. Zhang, *ACS Catal.* 2018, **8**, 5869-5874.
13. J. Lee, O. K. Farha, J. Roberts, K. A. Scheidt, S. T. Nguyen and J. T. Hupp, *Chem. Soc. Rev.* 2009, **38**, 1450-1459.
14. C. Bai, A. Li, X. Yao, H. Liu and Y. Li, *Green Chem.* 2016, **18**, 1061-1069.
15. G. Calleja, R. Sanza, G. Orcajo, D. Brionesa, P. Leob and F. Martínezb, *Catal. Today*. 2014, **227**, 130-137.
16. T. Toyao, M. Saito, Y. Horiuchi and M. Matsuoka, *Catal. Sci. Technol.* 2014, **4**, 625-628.
17. C. M. McGuirk, M. J. Katz, C. L. Stern, A. A. Sarjeant, J. T. Hupp, O. K. Farha and C. A. Mirkin, *J. Am. Chem. Soc.* 2015, **137**, 919-925.
18. J. Canivet, S. Aguado, C. Daniel and D. Farrusseng, *Chemcatchem*. 2011, **3**, 675-678.
19. S. Aguado, J. Canivet, Y. Schuurman and D. Farrusseng, *J. Catal.* 2011, **284**, 207-214.

20. M. Joharian, S. Abedi, A. Morsali, *Ultrason. Sonochem.* 2017, **39**, 897–907.
21. S. Ernst, M. Hartmann, S. Sauerbeck and T. Bongers, *Appl. Catal. A*, 2000, **200**, 117–123.
22. K. Narasimharao, M. Hartmann, H. H. Thiel and S. Ernst, *Micropor. Mesopor. Mat.* 2006, **90**, 377–383.
23. L. F. Tietze, *Chem. Rev.* 1996, **96**, 115–136.
24. M. Y. Masoomi, S. Beheshti, A. Morsali, *Cryst. Growth Des.* 2015, **15** (5), 2533–2538.
25. Y. Wang, L. Wang, C. Liu, R. Wang, *ChemCatChem.* 2015, **7**, 1559–1565.
26. M. Ohashi, M. P. Kapoor, S. Inagaki, *Chem. Commun.* 2008, **7**, 841–843.
27. U. P. N. Tran, K. K. A. Le, N. T. S. Phan, *ACS Catal.* 2011, **1**, 120–127.
28. M. Y. Masoomi, S. Beheshti, A. Morsali, *J. Mater. Chem. A*, 2014, **2**, 16863–16866.
29. B. Karmakar, B. Chowdhury and J. Banerji, *Catal. Commun.* 2010, **11**, 601–605.
30. J. Mondal, A. Modak, A. Bhaumik, *J. Mol. Catal. A: Chem.* 2011, **335**, 236–241.
31. L. Martins, W. Hölderich, P. Hammer, D. Cardoso, *J. Catal.* 2010, **271**, 220–227.
32. D. Tahmassebi, J. A. Wilson, J. M. Kieser, *Synth., Commun.* 2009, **39**, 2605–2613.
33. A. Zhu, R. Liu, L. Li, L. Li, L. Wang, J. Wang, *Catal. Today.* 2013, **200**, 17–23.
34. S. Neogi, M.K. Sharma, P.K. Bharadwaj, *J. Mol. Catal. A: Chem.* 2009, **299**, 1–4.
35. S. Saravanamurugan, M. Palanichamy, M. Hartmann, V. Murugesan, *Appl. Catal., A*, 2006, **298**, 8–15.
36. X. Zhang, E. S. Man Lai, R. Martin-Aranda, K. L. Yeung, *Appl. Catal. A: General.* 2004, **261**, 109–118.
37. Y. Luan, Y. Qi, H. Gao, R. S. Andriamitantsoa, N. Zheng, G. Wang, *J. Mater. Chem. A*, 2015, **3**, 17320–17331.
38. Y.K. Hwang, D.-Y. Hong, J.-S. Chang, S.H. Jhung, Y.-K. Seo, J. Kim, A. Vimont, M. Daturi, C. Serre, G. Férey, *Angew. Chem. Int. Ed.* 2008, **47**, 4144–4148.
39. P. Serra-Crespo, E.V. Ramos-Fernandez, J. Gascon, F. Kapteijn, *Chem. Mater.* 2011, **23**, 2565–2572.
40. A. Karmakar, G.M.D.M. Rúbio, M. Fátima, C. Guedes da Silva, S. Hazra, A.J.L. Pombeiro, *Cryst. Growth Des.* 2015, **15** (9), 4185–4197.
41. J. A. Gladysz, et al. *Handbook of Fluorous Chemistry; Wiley/VCH: Weinheim, Germany*, 2004.
42. (a) P. T. Nyffeler, S. G. Durn, M. D. Burkart, S. P. Vincent, C.-H. Wong, *Angew. Chem., Int. Ed.* 2005, **44**, 192–212. (b) I. T. Horvath, J. Rabai, *Science.* 1994, **266**, 72.

43. T. Nishino, M. Meguro, K. Nakamae, M. Matsushita and Y. Ueda, *Langmuir*, 1999, **15**, 4321–4323.
44. T. Sun, G. Qing, B. Su and L. Jiang, *Chem. Soc. Rev.*, 2011, **40**, 2909–2921.
45. B. V. Harbuzaru, A. Corma, F. Rey, P. Atienzar, J. L. Jordá, H. García, D. Ananias, L. D. Carlos and J. Rocha, *Angew. Chem., Int. Ed.*, 2008, **47**, 1080–1083.
46. D. M. Ciurtin, Y.-B. Dong, M. D. Smith, T. Barclay and H.-C. zurLoye, *Inorg. Chem.*, 2001, **40**, 2825–2834.
47. G.M. Sheldrick, *Acta Cryst.* 2015. C71, 3-8.
48. J. Farrugia, *J. Appl. Cryst.* 2012, **45**, 849-854.
49. S. Singh Dhankhar, M. Kaur, and C. M. Nagaraja, *Eur. J. Inorg. Chem.* 2015, **2015** (34), 5669–5676.
50. V. A. Blatov, A. P. Shevchenko, and D. M. Proserpio, *Crystal Growth & Design*. 2014, **14** (7), 3576-3586
51. Ch. Bonneau, M. O’Keeffe, D. M. Proserpio, V. A. Blatov, S. R. Batten, S. A. Bourne, M. Soo Lah, J.-Guillaume Eon, S. T. Hyde, S. B. Wiggin, and L. Öhrström, *Crystal Growth & Design*. 2018, **18** (6), 3411-3418.
52. <http://toris.topospro.com/>
53. J-Q Liu, Y-Y Wang, Zh-B Jia, *Inorg. Chem. Commun.* 2011, **14**, 519–521.
54. J. Li, Y. Peng, H. Liang, Y. Yu, B. Xin, G. Li, Z. Shi, and S. Feng, *Eur. J. Inorg. Chem.* 2011, **2011**, 2712–2719.
55. J. Zhou, Y. Wang, L Qin, M. Zhang, Q. Yang and H. Zheng, *CrystEngComm.* 2013, **15**, 616-627.
56. B.K. Tripuramallu, P. Manna, S.N. Reddy, S.K. Das, *Crystal Growth & Design*. 2012, **12**, 777-792.
57. M.Y. Masoomi, M. Bagheri, A. Morsali, P.C. Junk, *Inorg.Chem.Front.* 2016, **3**, 944-951.
58. C. Xu, W. Chu, S. Lei, X. Yang, *Z.Kristallogr.-New Cryst.Struct.* 2016, **231**, 907-909.
59. Y-X. Zhang, J. Yang, W-Q. Kan, J-F. Ma, *CrystEngComm.* 2012, **14**, 6004-6015.
60. M.Y. Masoomi, K.C. Stylianou, A.Morsali, P.Retailleau, D.Maspoch, *Crystal Growth & Design*. 2014, **14**, 2092-2096.
61. A.de O. Legendre, A.E. Mauro, V.M. Nogueira, E.E. Castellano, *Anal. Sci.:X-Ray Struct.Anal.Online.* 2008, **24**, x69- x70.

62. L. Carlucci, G. Ciani, D. M. Proserpio, T.G. Mitina, V.A. Blatov, *Chem. Rev.* 2014, **114** (15), 7557–7580.
63. E.V. Alexandrov, V.A. Blatov and D.M. Proserpio, *CrystEngComm*, 2017, **19**, 1993–2206.
64. a) H. J. Choi, M. Dinca, A. Dailly, J. R. Long, *Energy Environ. Sci.* 2010, **3**, 117–123; b) K. A. Cychosz, A. J. Matzger, *Langmuir*. 2010, **26**, 17198–17202; c) T. Wu, L. Shen, M. Luebbbers, C. Hu, Q. Chen, Z. Ni, R. I. Masel, *Chem. Commun.* 2010, **46**, 6120–6122; d) Y. Yoo, V. Varela-Guerrero, H. K. Jeong, *Langmuir*. 2011, **27**, 2652–2657.
65. J. B. Decoste, G. W. Peterson, M. W. Smith, C. A. Stone, C. R. Willis, *J. Am. Chem. Soc.* 2012, **134**, 1486–1489; b) J. Yang, A. Grzech, F. M. Mulder, T. J. Dingemans, *Chem. Commun.* 2011, **47**, 5244–5246.
66. X.-M. Lin, T.-T. Li, L.-F. Chen, L. Zhang and C.-Y. Su, *Dalton Trans.* 2012, **41**, 10422–10429.
67. S. Hasegawa, S. Horike, R. Matsuda, S. Furukawa, K. Mochizuki, Y. Kinoshita and S. Kitagawa, *J. Am. Chem. Soc.* 2007, **129**, 2607–2614.
68. M. K. Sharma, P. P. Singh and P. K. Bharadwaj, *J. Mol. Catal. A: Chem.* 2011, **342–343**, 6–10.
69. R. K. Das, A. Aijaz, M. K. Sharma, P. Lama and P. K. Bharadwaj, *Chem.–Eur. J.* 2012, **18**, 6866–6872.
70. J-Si Wang, F-Zheng Jin, H-Chao Ma, X-Bo Li, M-Yang Liu, J-Lan Kan, G-Jun Chen, and Y-Bin Dong, *Inorg. Chem.* 2016, **55** (13), 6685–6691.
71. R. A. Agarwal, S. Mukherjee, *Polyhedron*, 2016, **105**, 228–237.
72. A. Schejn, T. Mazet, V. Falk, L. Balan, L. Aranda, G. Medjahdi and R. Schneider, *Dalton Trans.* 2015, **44**, 10136–10140.